Influence of geotextile encasement in triaxial tests on gravel

Influence de l'enrobage de géotextile sur des essais triaxiaux sur gravier

Marina Miranda
School of Engineering and The Built Environment, Napier University, U.K, M.Miranda@napier.ac.uk

Almudena da Costa, Jorge Castro, César Sagaseta, Jorge Cañizal
Department of Ground Engineering and Materials Science, University of Cantabria, Spain

ABSTRACT: Stone columns installed in extremely soft soils may significantly reduce the effectiveness of this treatment due to the insufficient lateral confinement provided by the soft soil. The encasement of columns with geotextiles is commonly used in these situations with satisfactory results thanks to the extra confinement provided by the geotextile to the column. Drained triaxial tests on encased and non-encased samples of gravel have been performed to study the influence of the encasement on the behavior of stone columns. Two different densities of the gravel and two different geotextiles were used. The study is focused on the increase in strength of encased samples compared with non-encased ones, the extra confining pressure provided by the geotextiles and the mobilized friction angle of the gravel. In this paper, the results of some of these laboratory tests are compared with numerical simulation. All of the results show the improvement achieved when the gravel is encased with the geotextiles.

RÉSUMÉ : Les colonnes ballastées installées dans des sols extrêmement doux peuvent réduire significativement l'efficacité de ce traitement en raison du confinement latéral insuffisant fourni par le sol mou. L'encaissement des colonnes avec des géotextiles est couramment utilisé dans ces situations avec des résultats satisfaisants grâce au confinement supplémentaire fourni par le géotextile à la colonne. Des essais triaxiaux drainés sur des échantillons de gravier encastrés et non encastrés ont été réalisés pour étudier l'influence de l'encaissement sur le comportement des colonnes de pierre. Deux densités différentes du gravier et de deux géotextiles différents ont été utilisées. L'étude porte sur l'augmentation de la résistance des échantillons encastrés par rapport aux non encapsulés, la pression de confinement supplémentaire fournie par les géotextiles et l'angle de friction mobilisé du gravier. Dans cet article, les résultats de certains de ces tests de laboratoire sont comparés à la simulation numérique. Tous les résultats montrent l'amélioration obtenue lorsque le gravier est enveloppé avec les géotextiles.

KEYWORDS: gravel column, encased column, triaxial compression test, numerical analysis.

1 INTRODUCTION

Stone columns with granular material are often used to improve bearing capacity, to accelerate the speed of consolidation and to reduce settlements on soft soil strata. Insufficient lateral support in extremely soft soils (s_u<15 kPa) results in a significant reduction in the effectiveness of this treatment with stone columns. This lack of lateral confinement mainly occurs at shallow depths, causing bulging failure in the upper portion of the columns (e.g., Huges and Withers, 1974; Madhav and Miura, 1994). In these cases, an improvement in stone column behavior can be further enhanced by encapsulating the column with a flexible sleeve (geotextile or geogrid), which can be a continuous sleeve or can be formed with a longitudinal union.

The behavior of encapsulated stone columns has been studied by numerous research initiatives through the development of experimental tests, theoretical and numerical analyses and field applications.

An important part of the experimental studies has been performed by small-scale laboratory tests, focusing on the analysis of load-settlement behavior (e.g., Black et al., 2007; Ghazavi and Afshar, 2013; Gniel and Bouazza, 2009; Malarvizhi and Ilamparuthi, 2007; Murugesan and Rajagopal, 2007, 2010). For these experimental studies, the sleeves were mainly fabricated with geotextiles with a longitudinal union, which was commonly made by an overlap of the fabric that was sewn (e.g., Murugesan and Rajagopal, 2007, 2010), by a glued overlap of the fabric (e.g., Gniel and Bouazza, 2009), or by overlapping the encasement by a nominal amount and relying on the interlock between the aggregate and the section of overlap (e.g., Gniel and Bouazza, 2010). In any case, this union creates a weak point that reduces the strength of the geotextile. Other experimental analyses are based on triaxial compression tests on encased samples, such as the work of Rajagopal et al. (1999), who tested samples of granular soil encased in single and multiple geocells using different types of geotextiles, Wu and Hong (2009), who carried out triaxial compression tests on reinforced and non-reinforced columns mainly to assess the influence of the encasement on the radial strains of the sample and on the deviator stress, or Najjar et al. (2010) on normally consolidated kaolin samples reinforced with single sand columns.

In addition to the experimental studies, several numerical analyses have been carried out to study various factors that influence the behavior of the encased columns, such as the stiffness of the encasement (e.g., Almeida et al., 2013; Chungsik, 2010; Khabbazian et al., 2010; Murugesan and Rajagopal, 2006), the stiffness parameters of the compacted stone (Lo et al., 2010), the encasement length (Keykhosropur et al., 2012), the shear-induced volumetric dilation of the fill material (Hong, 2012), the behavior under no monotonic loads (e.g., Prisco et al., 2006), or the influence of the finite element modeling approach (e.g., Yoo and Kim, 2009).

2 EXPERIMENTAL PROGRAM

Three series of triaxial tests were performed, the first one with samples of only gravel and the second and third ones with gravel encased with two different geotextiles. Each of the series was carried out with samples with two different relative densities of the gravel, D_r=50% and 80%.

2 .1 *Test materials*

Details about the properties of the materials employed in the tests can be found in Miranda and Da Costa (2016). Below is a summary of these properties.

Uniformly graded limestone gravel with particle sizes between 4 and 5 mm was employed for the laboratory tests. This material is the same as that employed in Cimentada et al. (2011) and Miranda et al. (2015) for the study of the behavior of soft soils improved with non-encased stone columns.

Two different geotextiles were used for column reinforcement, each made using a different flat fabric. Both geotextiles, along with the properties of both fabrics, were provided by Huesker Synthetic Gmbh. In both cases, the sleeve was prepared by cutting the fabric and preparing it in a cylindrical shape with a longitudinal union. It is important to note that, in real treatments, continuous sleeves without longitudinal unions are constructed with these fabrics such that this weak point does not exist.

The comparison of the numerical simulations with the laboratory tests is presented only for one of the geotextiles. Fig1 shows the load-strain behavior of both the fabric and geotextile1 (fabric+joint). Selected values from the curve of this geotextile are summarized in Table 1, along with the corresponding secant modulus.

More details about the properties of these geotextiles can be found in Miranda (2014).

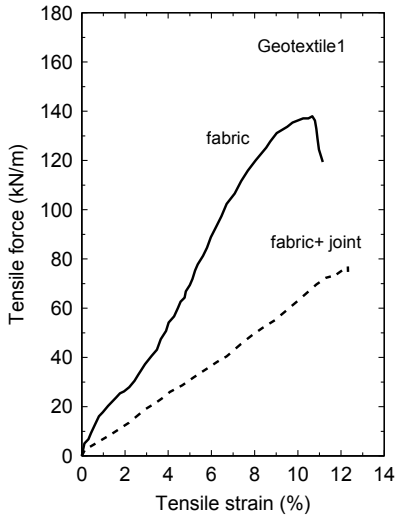

Figure 1. Tensile force versus strain of the geotextiles.

Table 1. Results of tensile tests. Geotextile1 (fabric+joint)

Strain [%]	Tension [kN/m]	Secant modulus Jg [kN/m]
2	13	650
5	31	620
8	50	625
Maximum 12.3	77	626

2 .2 *Specimen preparation*

The triaxial compression tests were performed on 200-mm-high x 100-mm-in-diameter specimens of only gravel and gravel encased with a geotextile. Two different dry unit weights of the gravel were used in the research, 14.5 kN/m^3 and 15.8 kN/m^3, which correspond to relative densities of D_r=50% and D_r=80%. The specimen preparation is described in Miranda and Da Costa (2016).

2 .3 *Test procedure*

Drained triaxial compression tests were conducted. The test procedure consisted of the following stages. First, the sample was saturated, and the desired confining pressure was applied with opened drainage until consolidation of the sample occurred. Four different confining pressures, p_c, of 25, 50, 150 and 300 kPa were chosen for the tests. Afterwards, the sample was axially loaded under a constant vertical strain rate of 0.002 mm/s, keeping the drainage open.

3 NUMERICAL ANALYSIS

Numerical analyses using the finite element software Plaxis 2D 2012 (Brinkgreve, 2012) were performed to simulate some of the triaxial tests performed in the laboratory. In particular, triaxial tests on samples encased with geotextile1 and with a relative density of gravel of D_r=50% were chosen for the numerical simulation.

The Hardening soil model (Schanz et al., 1999) was used to simulate the behavior of the gravel due to the stress dependency of the stiffness described in the experimental results. This model is an extension of the hyperbolic model developed by Duncan and Chang (1970), which is based on the theory of plasticity and includes soil dilatancy and introduces a yield cap. The strength of the soil in this model is given by the peak friction angle (ϕ) and the corresponding dilatancy (ψ). With these to values, the critical and mobilized friction angles, and the mobilized dilatancy are obtained by the following equations:

$$\sin\phi_{cr} = \frac{\sin\phi - \sin\psi}{1 - \sin\phi\sin\psi} \tag{1}$$

$$\sin\phi_m = \frac{\sigma_1' - \sigma_3'}{\sigma_1' + \sigma_3' - 2c\cot\phi} \tag{2}$$

$$\sin\phi_m < 3/4\sin\phi \rightarrow \psi_m = 0$$
$$\sin\phi_m > 3/4\sin\phi \text{ and } \psi > 0 \rightarrow \sin\psi_m = \max\left(\frac{\sin\phi_m - \sin\phi_{cr}}{1 - \sin\phi_m\sin\phi_{cr}}, 0\right) \tag{3}$$

Different stiffness and friction and dilatancy angles were employed for each of the four confining pressures used in the laboratory tests. These values were estimated from the experimental results (Fig. 2) and are summarized in Table 2.

Table 2. Gravel parameters for the numerical analyses

Chamber pressure, p_c [kPa]	Friction angle* [º]	Dilatancy [º]	E_{50}^{ref} [MPa]	E_{oed}^{ref} [MPa]
25	54	14	9.5	8.2
50	47	12	10.0	10.0
150	43	5	13.5	12.0
300	40	0	16.5	13.0

(*) peak values

The unloading-reloading stiffness was chosen as three times the secant stiffness. The values of the Poisson's ratio for each confining pressure have been obtained from the initial slope of the volume strain – axial strain curves (Fig. 2). A Poisson's ratio of 0.25 was obtained for the chamber pressures of 25 and 50 kPa and 0.15 for chamber pressures of 150 and 300 kPa. The best numerical analysis fit with the experimental results was obtained for a power for stress dependency of the stiffness of m=0.2.

Grid elements were used to represent the geotextile. The stiffness is the only parameter required for this material, and a value of 620 kN/m was adopted for the calculations.

Two calculation phases were defined in the numerical model in Plaxis to simulate the triaxial tests with the encased samples. The first one was a consolidation calculation in which the chamber pressure is applied to the sample. During the second one, the axial stress is increased until a certain value that, for each chamber pressure, was chosen as the maximum value reached in the laboratory tests.

4 RESULTS

Results from the laboratory tests can be found in Miranda and Da Costa (2016). The results presented in this section are focused on the comparision between the laboratory and the numercial results.

4 .1 *Gravel specimens*

The numerical simulation of the consolidated-drained triaxial compression tests on non-encased samples was performed using the Soil Test facility in Plaxis. The numerical results are given in 2, and they show a good fit with the experimental results.

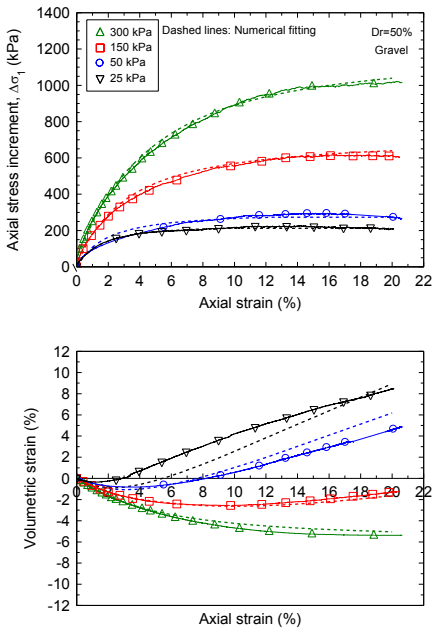

Figure 2. Numerical fitting of the drained triaxial tests of the gravel

4 .2 *Encased gravel specimens*

The results of the axial stress increment and the volumetric strain against the axial strain are presented in Fig. 3, along with those from the numerical analyses.

Comparing the results for non-encased and encased samples the following conclusions are obtained. For low axial strains, the behavior of encased and non-encased samples is similar, with no influence of the geotextile. This is attributed to the volume change of the sample during the defrosting process and isotropic consolidation. This volume change reduces the diameter of the sample such that it is slightly smaller than the diameter of the encasement; therefore, some axial strain is needed so that the sample is in contact with the encasement. This is not constant along the sample, so the process takes place progressively. Once the contact is reached, at different axial strains depending on the gravel density and the chamber pressure, the influence of the encasement becomes noticeable. The geotextile develops increasing tensile force and increasing circumferential strain that lead to a continuous increase of axial stress, which is supported by the high stiffness of the geotextiles, resulting in higher axial stress increments for the encased samples compared with the non-encased ones (only gravel). The noticeable influence of the confining pressure in the results of the non-encased samples is not so noticeable in the results of the encased ones.

The strain hardening behavior observed in the stress-strain curves of encased samples is attributed to the mobilization of the geotextile strength. During the test, increasing radial and circumferential strains are developed. As a consequence, in encased samples, the geotextile develops an increasing circumferential tensile force per unit length, the value of which depends on the stiffness of the geotextile. This increase in the circumferential tensile force of the geotextile results in an extra confining pressure provided by the encapsulating geotextile to the gravel, which is added to the chamber pressure applied for the test.

As was expected, the numerical results do not show the described initial behavior obtained in the laboratory tests where the influence of the geotextile is not realized until a certain axial strain is reached. The reason is that, in the numerical calculation, the geotextile develops radial strain from the beginning of the second calculation phase, whereas in the laboratory tests, some axial strain is needed to achieve a complete response of the geotextile. This is slightly noticeable in the axial stress increments, but it is clearly shown by the volumetric strain with a different initial response. However, if the numerical volumetric curves are horizontally translated to a certain axial strain, a good fit with the laboratory results is obtained.

Fig. 4 shows the ratio between the axial stress increments in encased and non-encased samples obtained from the numerical analysis and its comparison with the experimental results. The agreement of numerical and experimental results is quite satisfactory.

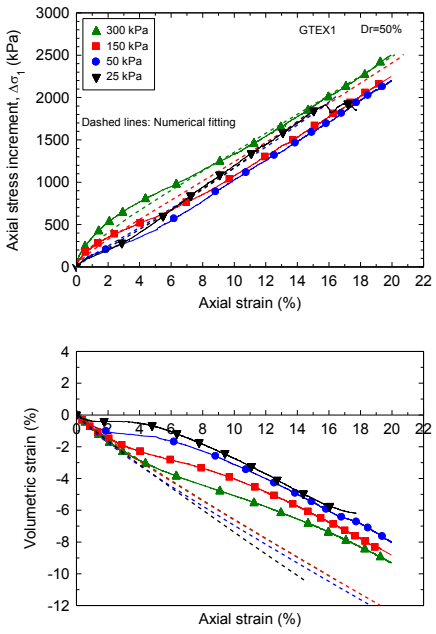

Figure 3. Numerical results of the drained triaxial tests in samples encased with geotextile1

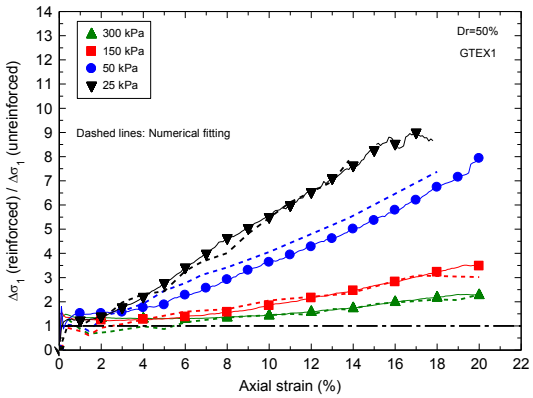

Figure 4. Numerical result for the ratio of axial stress increment (reinforced/unreinforced samples)

5 CONCLUSION

A series of consolidated-drained triaxial compression tests were performed to study the effectiveness of encapsulation on the strength of gravel columns.

The improvement in the strength of encased samples was evaluated by the ratio of the axial stress increment in the encased and the non-encased samples. This improvement is more significant for low confining pressures with a value of 9.5 for p_c=25 kPa at an axial strain of 17% and 2.5 for p_c =300 kPa.

Numerical analyses were conducted for comparison with the experimental results. This comparison was performed for samples encased with geotextile1 and with D_r=50%. The numerical simulation matches the laboratory test results quite well except for the initial behavior where the influence of the geotextile is not realized in the laboratory tests until a certain axial strain has been developed.

6 ACKNOWLEDGEMENTS

The authors would like to thank HUESKER Synthetic GmbH Company for providing the geotextiles needed for the encasement and their properties.

7 REFERENCES

Almeida M. S. S., Hosseinpour I. and Riccio M. 2013. Performance of a geosynthetic-encased column (GEC) in soft ground: numerical and analytical studies. *Geosynthetics International* 20 (4), 252-262.

Black J. A., Sivakumar M. R., Madhav M. R. and Hamii, G. A. 2007. Reinforced stone columns in weak deposits: laboratory model study. J. *Geotechnical and Geoenvironmental Engineering* 133 (9), 1154-1161.

Brinkgreve R.B.J. 2012. *Plaxis finite element code for soil and rock analysis, 2D.* Rotterdam: Balkema.

Chungsik A.M. 2010. Performance of geosynthetic-encased stone columns in embankment construction: Numerical investigation. *J. Geotech. Geoenviron Eng.* ASCE. 136, 1148-1160.

Cimentada A., da Costa A., Cañizal J. and Sagaseta C. 2011. Laboratory study on radial consolidation and deformation in clay reinforced with stone columns. *Canadian Geotechnical Journal* 48(1), 36-52.

Duncan J.M. and Chang C.Y. 1970. Nonlinear analysis of stress and strain in soils. *J. Soil Mech. Found.* Div. ASCE 96 (5), 1629-1653.

Ghazavi M. and Afshar J.N. 2013. Bearing capacity of geosynthetic encased stone columns. *Geotextiles and Geomembranes* 38, 26-36.

Gniel J., Bouazza, A., 2009. Improvement of soft soils using geogrid encased stone columns. *Geotextiles and Geomembranes* 27 (3), 167–175.

Gniel, J. and Bouazza A. 2010. Construction of geogrid encased stone columns: A new proposal based on laboratory testing. *Geotextiles and Geomembranes* 28 (1), 108-118.

Hong Y.S. 2012. Performance of encased granular columns considering shear-induced volumetric dilation of the fill material. *Geosynthetics International* 19 (6), 438 –452.

Huges J.M.O. and Withers N.J. 1974. Reinforcing of cohesive soils with stone columns. *Ground Engineering* 7 (3), 42-49.

Khabbazian M., Kaliakin V.N. and Meehan C.L. 2010. Numerical study of the effect of geosynthetic encasement on the behaviour of granular columns. *Geosynthetics International* 17 (3), 132 –143.

Keykhosropur L., Soroush A. and Imam R. 2012. 3D numerical analyses of geosynthetic encased stone columns. *Geotextiles and Geomembranes* 35, 61-68.

Lo S.R., Zhang R. and Mak J., 2010. Geosynthetic-encased stone columns in soft clay: A numerical study. *Geotextiles and Geomembranes* 28 (3), 292-302.

Madhav M.R. and Miura N. 1994. Soil improvement. Panel report on stone columns. In: *Proceedings of the 13th International Conference on Soil Mechanics and Foundation Engineering*, New Delhi, India. 5, 163-164.

Malarvizhi S.N. and Ilamparuthi K. 2007. Comparative study on the behavior of encased stone column and conventional stone column. *Soils and Foundations* 47 (5), 873-885.

Miranda M. 2014. *Influencia de la densidad y del confinamiento con geotextil en columnas de grava*. PhD dissertation. Spain. University of Cantabria.

Miranda M. and Da Costa A. 2016. Laboratory analyses of encased stone columns. *Geotextiles and Geomembranes* 44 (3), 269-277.

Miranda M., Da Costa A., Castro J. and Sagaseta C. 2015. Influence of gravel density in the behaviour of soft soils improved with stone columns. *Canadian Geotechnical Journal*, 52 (12), 1968-1980.

Murugesan S. and Rajagopal K. 2006. Geosynthetic-encased stone columns: numerical evaluation. *Geotextiles and Geomembranes* 24 (6), 349-358.

Murugesan S. and Rajagopal K. 2007. Model tests on geosynthetic-encased stone columns. *Geosynthetics International* 14 (6), 346-354.

Murugesan S. and Rajagopal K. 2010. Studies on the behavior of single and group of geosynthetic encased stone columns. . *J. Geotechnical and Geoenvironmental Engineering* 136 (1), 129-139.

Najjar S., Sadek,S. and Maakaroun T. 2010. Effect of sand columns on the undrained load response of soft clays. *J. Geotech. Geoenviron. Eng.* ASCE, 136(9), 1263–1277.

Prisco C., Galli A., Cantarelli E.and Bongiorno D. 2006. Geo-reinforced sand columns: small scale experimental tests and theoretical modeling. *Proc. of 8th International conference of Geosynthetics*. Yokahama. 1685-1688.

Rajagopal K., Krishnaswamy N.R. and Madhavi Latha G., 1999. Behavior of sand confined with single and multiple geocells. *Geotextile and Geomembranes* 17 (3), 171-184.

Schanz T., Vermeer P. and Bonnier P. 1999. The hardening soil model: formulation and verification. *Proc. Plaxis Symp. Beyond 2000 in computational geotechnics* Amsterdam, Balkema.

Yoo, C., Kim, S.B., 2009. Numerical modeling of geosynthetic-encased stone column-reinforced ground. Geosynthetics International 16 (3), 116 –126.

Wu, C.S., Hong, Y.S., 2009. Laboratory tests on geosynthetic-encapsulated sand columns. *Geotextile and Geomembranes* 27 (2), 107-120.